Pressure-temperature phase diagram for charge-transfer transition in $Cs[Co(3\text{-}CNpy)_2][W(CN)_8]H_2O$

J. E. Kim and Y. Ohishi
JASRI/SPring-8, 1-1-1 Kouto, Sayo-cho, Sayo-gun, Hyogo 679-5198, Japan

Y. Moritomo*
Department of Physics, University of Tsukuba, Tsukuba 305-8571, Japan

K. Kato and M. Takata
RIKEN SPring-8 Center, 1-1-1 Kouto, Sayo-cho, Sayo-gun, Hyogo 679-5148, Japan

S. Ohkoshi
Department of Chemistry, University of Tokyo, Tokyo 113-0033, Japan

(Received 6 July 2007; revised manuscript received 12 September 2007; published 22 January 2008)

Effects of the hydrostatic pressure on the magnetic and structural properties are investigated in a charge-transfer material, $Cs[Co(3\text{-}CNpy)_2][W(CN)_8]H_2O$ (CNpy=cyanopyridine), with two-dimensional Co-W network bridged by CN anions. We have found that the compound shows a pressure-induced charge-transfer (CT) transition at 0.5 GPa at room temperature, accompanied by a remarkable color change from transparent red to green. The upper critical temperature ($T_{CT,up}$) for the CT transition increases at a huge rate of 250 K/GPa under pressures, reflecting the concomitant significant volume change ($\Delta V/V=0.08$).

DOI: 10.1103/PhysRevB.77.012101 PACS number(s): 64.70.K−, 61.50.Ks, 75.30.Kz, 81.30.−t

A cooperative charge transfer (CT) is frequently observed in coordination compounds, such as halogen-bridged gold complex, $Cs_2Au_2X_6$ (X=I, Br, Cl),[1] and several cyano-bridged metal complexes.[2,3] In these charge-transfer compounds, the metal ions are bridged by halogens or cyano moieties as -*A*-NC-*B*-CN-*A*-NC-*B*-, where *A* and *B* are the metal ions. The cooperative charge transfer, e.g., $-A^{2+}$-NC-B^{3+}- and $-B^{3+}$-NC-A^{2+}-, alters the spin state as well as the ionic radius of the metal ions and hence changes the magnetic and structural properties of the system. Furthermore, the CT transition can be induced not only by heating and/or cooling but also by the external field, such as the photoexcitation,[4–11] the hydrostatic pressure,[12] and the x-ray irradiation.[13] Among the external fields, the hydrostatic pressure is a "clean" perturbation that is free from inhomogeneity and modifies the structural parameters that govern the phase stability.[14–18] In this sense, a structural investigation is essential for the quantitatively comprehension of the pressure effects. Here, we performed an integrated investigation of the pressure effects on the CT transition.

The target charge-transfer material is $Cs[Co(3\text{-}CNpy)_2]\times[W(CN)_8]H_2O$, with two-dimensional (2D) Co-W network bridged by CN anions. Among the eight CN moieties of the octacyanotungsten ($[W(CN)_8]$), four are linked to the neighboring Co atoms to form a zigzag sheet, which stacks along the *b* direction in the triclinic ($P\bar{1}$, $Z=2$) setting.[9] The Co site is surrounded by six NC^- groups, and it is suffered by the ligand field. The W-C bond distance (average of the eight independent bond distances) and the Co-N bond distance (average of the three independent bond distances) are 2.141 and 2.126 Å at 298 K, respectively.[9] With decrease of temperature, the compound shows the thermally induced CT transition at $T_{CT,down}=140$ K from the Co^{2+} ($S=\frac{3}{2}$)-W^{5+} ($S=\frac{1}{2}$) configuration to the Co^{3+} ($S=0$)-W^{4+} ($S=0$) configuration. The Co–W bond distance $d_{Co\text{-}W}$ (average of the four independent bond distances) significantly decreases from 5.362(3) Å at 300 K to 5.155(2) Å at 100 K.[10] The longer Co–W bond distance in the high-temperature phase would reduce the ligand field on the Co^{2+} ion and stabilize the high-spin (HS) Co^{2+} state.[19] At the CT transition, the compound shows a significant color change from transparent red to green. Arimoto *et al.*[9] have found that photoirradiation of a visible light (wavelength is 600–750 nm and excitation power is 12.5 mW cm^{-2}) at 5 K induces magnetization and ascribed the phenomenon to the photoinduced CT transition. This scenario is further confirmed by the x-ray absorption fine structure spectroscopy[11] as well as the x-ray powder structural analysis.[10]

In this Brief Report, we have derived the pressure-temperature (*P*-*T*) phase diagram for the CT transition of $Cs[Co(3\text{-}CNpy)_2][W(CN)_8]H_2O$. We have found that the upper critical temperature ($T_{CT,up}$) for the CT transition increases at a huge rate of 250 K/GPa under pressures, reflecting the concomitant significant volume change ($\Delta V/V=0.08$). Based on the systematic structural investigation against temperature and pressure, we have quantitatively separated the intrinsic *entropy* effect induced by temperature from the conventional *lattice* effect or the thermal expansion effect.

Red powders of the compound were prepared by adding an aqueous solution of $Cs_3[W(CN)_8]$ (0.1 mol/l) to a mixed aqueous solution of $CoCl_2$ (0.1 mol/l) and 3-CNpy (0.2*M*) at room temperature. Details of the sample characterization were described elsewhere.[9]

Figure 1 shows the pressure-induced color change of the compound, measured in a gasket whole of a diamond anvil cell at 300 K. Magnitude of the applied pressure was monitored by the wavelength of the luminescence line R_1 (Ref.

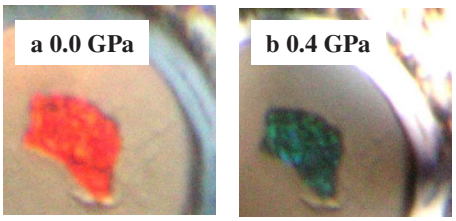

FIG. 1. (Color online) Room-temperature microscope image of $Cs[Co(3\text{-}CNpy)_2][W(CN)_8]H_2O$ within the diamond anvil cell at (a) ambient pressure and (b) at 0.44 GPa. The color change is reversible in the repeated pressure cycles.

20) from a small piece of ruby placed in the gasket hole. The sample color changes from transparent red to green at $P=0.44$ GPa in the pressure-increasing run, while the reverse change is observed at $P=0.30$ GPa in the pressure-decreasing run. The color change is ascribed to the pressure-induced CT transition from the Co^{2+}-W^{5+} configuration to the Co^{3+}-W^{4+} configuration, and it is reversible for the repeated pressure cycles. The transparent red color is originated in the weak absorption at 500 nm due to the dipole-forbidden *d-d* transition of the Co^{2+} ions.[21] On the other hand, the green color can be ascribed to the rather intense absorption at 840 nm due to the charge-transfer excitation from the W^{4+} site to the Co^{3+} site. Hereafter, we will call these phases simply as the "red" phase and the "green" phase, respectively.

Next, we have investigated the magnetic susceptibility χ under hydrostatic pressures, with a piston-cylinder-type pressure cell and a squid type magnetometer (Quantum Design; magnetic property measurement system). The sample powders (5.6 mg) were sealed in the cylinder, 2 mm in diameter, with a Daphne 7373 oil (made by Idemitsu) as a pressure-transmitting medium. In order to estimate the χ value of the sample, we subtracted background magnetic response (of the empty pressure cell) from the total response (of the pressure cell with sample). The unexpected behavior of χ at $P=0.5$ GPa is due to the imperfect subtraction. The applied magnetic field was 1000 Oe and the cooling and warming rate was set at ± 1 K/min. The whole pressure-induced change in χ was reversible for the repeated pressure cycles.

At ambient pressure (lowest curve in Fig. 2), the magnetic susceptibility shows distinct reduction at the lower critical temperature $T_{CT,down}$ (=134 K) in the cooling run. This reduction of χ can be ascribed to the CT transition from the magnetic Co^{2+}-W^{5+} configuration (red phase) to the nonmagnetic Co^{3+}-W^{4+} configuration (green phase). The rise of the low-temperature region ($\leqslant$100 K) may be ascribed to the residual red phase domains induced by the slight pressure inhomogeneity within the pressure cell. Here, note that the residual red phase domain is absent when the sample is out of the pressure cell and the pressure-transmitting medium.[9] The residual phase shows ferromagnetism below 30 K, and volume fractions of the residual phase are 0.09 at 0.0 GPa, 0.10 at 0.1 GPa, 0.04 at 0.2 GPa, 0.03 at 0.3 GPa, 0.02 at 0.04 GPa, and 0.02 at 0.5 GPa. The CT transition shows a significant thermal hysteresis, and the compound becomes magnetic again above the upper critical temperature $T_{CT,up}$ (=206 K) in the warming run. Application of pressure pushes

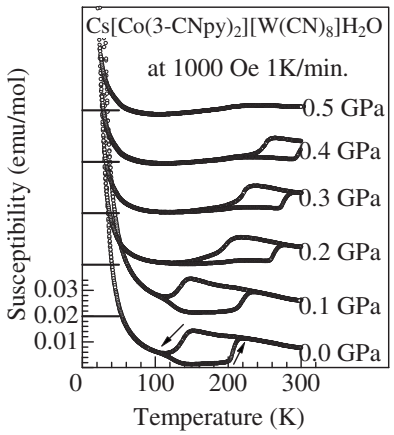

FIG. 2. Temperature dependence of the magnetic susceptibility of $Cs[Co(3\text{-}CNpy)_2][W(CN)_8]H_2O$ under various pressures. Arrows represent the direction of the measurement.

up both the critical temperatures, i.e., $T_{CT,up}$ and $T_{CT,down}$. Eventually, the red phase disappears at $P=0.5$ GPa. The effective magnetic moment μ_{eff} is estimated to be $4.4\mu_B$ per a Co-W pair at ambient pressure, which is close to the calculated value ($=5.2\mu_B$) for the independent $S=\frac{3}{2}$ and $S=\frac{1}{2}$ spins. We estimate that the μ_{eff} by assuming the magnetic interaction between Co^{2+} and W^{3+} is negligible. This assumption is valid because the Curie temperature of the photocreated red phase is very low [=30 K (Ref. 9)], which is a measure for the magnetic interaction between them. The magnitude of μ_{eff} is nearly independent of pressure: $4.2\mu_B$ at 0.1 GPa, $4.3\mu_B$ at 0.2 GPa, $4.5\mu_B B$ at 0.3 GPa, and $4.4\mu_B$ at 0.44 GPa. This indicates that the spin states of the pressurized red phase are the same as at ambient pressure.

Based on thus obtained critical temperatures, we derived the *P-T* phase diagram (Fig. 3). The red phase is located in the high-*T* and low-*P* region, while the green phase is in the low-*T* and high-*P* region. The upper phase boundary steeply increases with pressure at a rate of $dT_{CT,up}/dP$

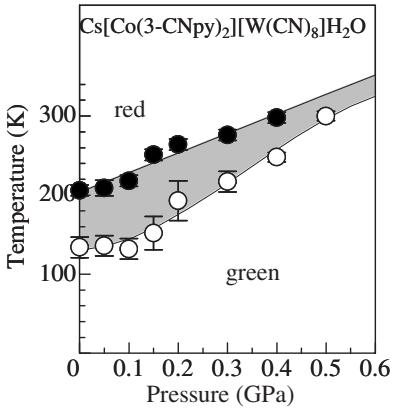

FIG. 3. Pressure-temperature phase diagram of $Cs[Co(3\text{-}CNpy)_2][W(CN)_8]H_2O$. Open and filled circles represent lower ($T_{CT,down}$) and upper ($T_{CT,up}$) critical temperatures, respectively. The electronic configuration of the red phase and the green phase are Co^{2+}-W^{5+} and Co^{3+}-W^{4+}, respectively. The hatched region is bistable.

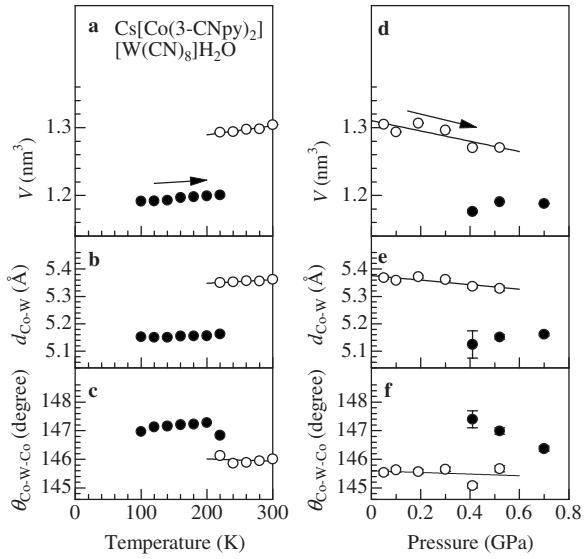

FIG. 4. Temperature dependence of (a) the unit cell volume V, (b) the Co–W bond distance $d_{\text{Co-W}}$ (average of the four independent bond distances), and (c) the Co–W–Co bond angle $\theta_{\text{Co-W-Co}}$ of $Cs[Co(3\text{-}CNpy)_2][W(CN)_8]H_2O$. Pressure dependence of (d) V, (e) $d_{\text{Co-W}}$, and (f) $\theta_{\text{Co-W-Co}}$ at 300 K. Arrows represent the direction of the measurement. The open and filled circles are for the red phase and the green phase, respectively. The double data points at 0.4 and 0.5 GPa indicate the coexistence of the two phases. The straight lines are the results of the least-squares fitting in the red phase.

$=250$ K/GPa. This huge pressure coefficient can be ascribed to the significant volume change ΔV ($=0.09$ nm^3; see Fig. 4) at the CT transition. Recall that the coefficient can be expressed by the so-called Clusius-Clapeyron equation as $dT_{\text{CT,up}}/dP=\Delta V/\Delta S$, where ΔS is the entropy change at the transition. Here, we point out that the large ΔV value is a characteristic of the CT transition of the cyano-bridged materials. Actually, a significant volume change is observed at the CT transitions in the $RbMn[Fe(CN)_6]$ [$\Delta V/V=0.11$ (Refs. 3 and 22)] and $Na_xCo_y[Fe(CN)_6]\cdot zH_2O$ [$\Delta V/V=0.11$ (Ref. 2)]. Such a large volume change is ascribed to the reduction of the ionic radius of the constituent metal ions, i.e., Mn^{3+} and Co^{3+}. In the present compound, the ionic radius r_{Co} of the Co ions decreases from 0.745 Å in the HS Co^{2+} to 0.545 Å in the LS Co^{3+}.[24] The resultant contraction of the Co–W bond distance, together with the 2D network structure, causes the significant volume change.

Now, let us proceed to the structural change induced by temperature and pressure. The structure of $Cs[Co(3\text{-}CNpy)_2][W(CN)_8]H_2O$ was determined by the Rietveld analysis of the x-ray powder diffraction patterns, obtained at the BL02B2 beamline[23] and the BL10XU beamlines at SPring-8. The red powders were carefully pulverized with a microspatula until the powders gave a homogeneous intensity distribution in the Debye-Scherrer powder ring, which is a necessary condition for the reliable Rietveld analysis. In the temperature dependent measurement at the BL02B2 beamline, the powders were sealed in a quartz capillary, 0.2 mm in diameter. The wavelength of the incident x ray was 0.826 88 Å and the exposure time was 5 min. The 2θ range used in the Rietveld analysis is 2°–70°. In the pressure dependent measurement at the BL10XU beamline, the powders were sealed in a gasket hole of the diamond anvil cell, about 0.1 mm in thickness and about 0.3 mm in diameter, which was filled with the Daphne 7373 oil as a pressure-transmitting medium. The wavelength of the incident x ray was 0.621 95 Å. The 2θ range used in the Rietveld analysis is 2°–30°. Magnitude of the applied pressure was monitored by the wavelength of the luminescence line R_1 (Ref. 20) from a small piece of ruby placed in the gasket hole. In order to avoid the irradiation damage,[10] the exposure time (=1 min) was set to be short and the sample position was changed at every measurement. The Rietveld analysis was performed with a triclinic ($P1$; $Z=2$) space group with rigid molecular units of CN-, H_2OCs, and 3-CNpy. In the vicinity of the phase boundary [at 220 K at ambient pressure in Fig. 3(a) and at 0.41 and 0.52 GPa at 300 K in Fig. 3(d)], a two phase model was adopted. The reliable factors, R_{wp} (R_{I}), are in the range of 0.028–0.047 (0.059–0.080).

In Fig. 4, we plotted the prototypical structural parameters, i.e., V, $d_{\text{Co-W}}$, and the Co–W–Co bond angle $\theta_{\text{Co-W-Co}}$, as a function of temperature [Figs. 4(a)–4(c)] and applied pressure [Figs. 4(d)–4(f)]. Especially, the latter two parameters determine the size and the shape of the Co-W sheets, which is the platform stage for the cooperative CT transition. With increase of temperature, the magnitude of V discontinuously increases from 1.20 to 1.29 nm^3 [Fig. 4(a)] at 210 K, which corresponds to the relative volume change $\Delta V/V$ of 0.08. The application of pressure, on the other hand, gradually decreases V [Fig. 4(d)], and eventually the phase transition to the green phase takes place at 0.4–0.5 GPa. This value is consistent with the value ($P_{\text{CT}}=0.5$ GPa) obtained by the magnetic measurement. The magnitude of $\Delta V/V$ is 0.07 for the pressure-induced CT transition at 300 K. In order to quantitatively compare the pressure-induced structural change and the temperature-induced structural change, we calculated the temperature and pressure coefficient of these parameters [see the straight lines in Figs. 4(a)–4(f)]: $dV/dT=1.3\times10^{-4}$ nm^3/K, $dd_{\text{Co-W}}/dT=1.3\times10^{-4}$ Å/K, $d\theta_{\text{Co-W-Co}}/dT=-7.5\times10^{-4}$ deg/K, $dV/dP=-7.5\times10^{-2}$ nm^3/GPa, $dd_{\text{Co-W}}/dP=-8.3\times10^{-2}$ Å/GPa, and $d\theta_{\text{Co-W-Co}}/dP=-2.8°$/GPa. Here, we emphasize that the relative change of $\theta_{\text{Co-W-Co}}$ is one order smaller than the other two parameters. We found that the ratio of dV/dT and dV/dP is nearly the same as that of $dd_{\text{Co-W}}/dT$ and $dd_{\text{Co-W}}/dP$. So, we concluded that the structural change induced by 1 GPa pressure corresponds to that induced by the temperature drop of 600 K.

Finally, let us discuss the roles of the temperature on the CT transition. The most important role of the temperature is to increase the entropy term in the free energy function, which causes the phase transition into the high-entropy state (red phase) with increase of temperature. In addition to this entropy effect, the actual compound shows the thermal expansion with temperature. We call this temperature effect as "lattice" effect, which modifies the material parameters that govern the phase stability. Here, let us consider the warming process from $T_{\text{CT,down}}$ (=134 K at 0 GPa) to 300 K at ambient pressure. Using the scaling relation discussed above, the thermal expansion ($\Delta T=166$ K) is compensated by the external pressure of ≈0.3 GPa. On the other hand, the external

pressure of 0.5 GPa is needed to induce the CT transition at 300 K. Then, the extra pressure ($\approx$0.2 GPa) compensates the enhanced entropy effect at 300 K. In other words, the ratio of the lattice effect and the entropy effect is $\approx 3:2$ for the present compound. Thus, we can distinguish the two thermal effects, i.e., the lattice effect and the entropy effect by the systematic structural analysis. Our structural approach is applicable to the P-T phase diagram of the other material.

In summary, we have derived the P-T phase diagram for the CT transition of $Cs[Co(3\text{-}CNpy)_2][W(CN)_8]H_2O$. The significant volume change ($\Delta V/V=0.08$) at the CT transition is responsible for the huge pressure sensitivity ($dT_{CT,up}/dP = 250$ K/GPa). The pressure control of the CT transition, which strongly couples with the spin and lattice degree of freedom, is a promising approach to create a room-temperature functionality.

This work was supported by a Grant-in-Aid for Scientific Research from the Ministry of Education, Culture, Sports, Science and Technology, Japan and from Japan Science and Technology Agency (CREST "X-ray Pinpoint Structural Measurement: Development of the spatial- and time-resolved structural study technique for nanomaterials and devices"). The synchrotron-radiation x-ray powder experiments were performed at the SPring-8 BL02B2 and BL10XU with the approval of the Japan Synchrotron Radiation Research Institute (JASRI).

*Corresponding author.

[1] N. Kojima, M. Hasegawa, H. Kitagawa, and O. Shimomura, J. Am. Chem. Soc. **1116**, 11368 (1994).
[2] N. Shimamoto, S. Ohkoshi, O. Sato, and K. Hashimoto, Inorg. Chem. **41**, 678 (2002).
[3] S. Ohkoshi, H. Tokoro, M. Utsunomiya, M. Mizuno, M. Abe, and K. Hashimoto, J. Phys. Chem. **106**, 2423 (2002).
[4] O. Sato, T. Iyoda, A. Fujishima, and K. Hashimoto, Science **272**, 704 (1996).
[5] O. Sato, Y. Einaga, T. Iyoda, A. Fujishima, and K. Hashimoto, J. Electrochem. Soc. **144**, L11 (1997).
[6] O. Sato, Y. Einaga, A. Fujishima, and K. Hashimoto, Inorg. Chem. **38**, 4405 (1999).
[7] A. Goujon, F. Varret, V. Escat, A. Bleuzen, and M. Verdauguer, Polyhedron **20**, 1339 (2001).
[8] X. J. Liu, Y. Moritomo, M. Ichida, A. Nakamura, and N. Kojima, Phys. Rev. B **61**, 20 (2000).
[9] Y. Arimoto, S. Ohkoshi, Z. J. Zhong, H. Sekine, Y. Mizobe, and K. Hashimoto, J. Am. Chem. Soc. **125**, 9240 (2003).
[10] J. E. Kim, Y. Ohishi, Y. Moritomo, K. Kato, M. Takata, and S. Ohkoshi, Phys. Rev. B **76**, 014106 (2007).
[11] T. Yokoyama, K. Okamoto, T. Ohta, S. I. Ohkoshi, and K. Hashimoto, Phys. Rev. B **65**, 064438 (2002).
[12] Y. Moritomo, M. Hanawa, Y. Ohishi, K. Kato, M. Takata, A. Kuriki, E. Nishibori, M. Sakata, S. Ohkoshi, H. Tokoro, and K. Hashimoto, Phys. Rev. B **68**, 144106 (2003).
[13] S. Margadonna, K. Prassides, and A. D. N. Fitch, Angew. Chem., Int. Ed. **43**, 6316 (2004).
[14] V. Ksennofontov, A. B. Gaspar, J. A. Real, and P. Gútlich, J. Phys. Chem. B **105**, 12266 (2001).
[15] M. Takano, S. Nasu, T. Abe, K. Yamamoto, S. Endo, Y. Takeda, and J. B. Goodenough, Phys. Rev. Lett. **67**, 3267 (1991).
[16] P. Gútlich, V. Ksennofontov, and A. B. Gaspar, Coord. Chem. Rev. **249**, 1811 (2005).
[17] E. Coronado, M. C. Giménez-López, G. Levchenko, F. M. Romero, V. Garcia-Baonza, A. Milner, and M. Paz-Pasternak, J. Am. Chem. Soc. **127**, 4580 (2005).
[18] A. Mitsuda, T. Goto, K. Yoshimura, W. Zhang, N. Sato, K. Kosuge, and H. Wada, Phys. Rev. Lett. **88**, 137204 (2002).
[19] Based on our structural analysis, the Co-N bond distance increses from 2.011(157) Å, at 100 K to 2.128(90) Å at 300 K.
[20] H. K. Mao, Science **200**, 1145 (1978).
[21] O. G. Holmes and D. S. McClure, J. Chem. Phys. **26**, 1686 (1957).
[22] K. Kato, Y. Moritomo, M. Takata, M. Sakata, M. Umekawa, N. Hamada, S. Ohkoshi, H. Tokoro, and K. Hashimoto, Phys. Rev. Lett. **91**, 255502 (2003).
[23] E. Nishibori, M. Takata, K. Kato, M. Sakata, Y. Kubota, S. Aoyagi, Y. Kuroiwa, M. Yamakawa, and N. Ikeda, Nucl. Instrum. Methods Phys. Res. A **467-468**, 1045 (2001).
[24] R. D. Shannon, Acta Crystallogr., Sect. A: Cryst. Phys., Diffr., Theor. Gen. Crystallogr. **32**, 1751 (1976).